Disconnected contribution to the LO HVP term of muon g-2 from ETMC

C. Alexandrou,^{a,b} **S. Bacchio,**^{b,*} **P. Dimopoulos,**^{c} **J. Finkenrath,**^{b} **R. Frezzotti,**^{d}
G. Gagliardi,^{e} **M. Garofalo,**^{f} **K. Hadjiyiannakou,**^{a,b} **B. Kostrzewa,**^{g} **K. Jansen,**^{h}
V. Lubicz,^{i} **M. Petschlies,**^{f} **F. Sanfilippo,**^{e} **S. Simula,**^{e} **C. Urbach**^{f} **and U. Wenger**^{j}

^{a}*Department of Physics, University of Cyprus, 20537 Nicosia, Cyprus*

^{b}*Computation-based Science and Technology Research Center, The Cyprus Institute,*
  20 Konstantinou Kavafi Street, 2121 Nicosia, Cyprus

^{c}*Dipartimento di Scienze Matematiche, Fisiche e Informatiche, Università di Parma and INFN, Gruppo*
  Collegato di Parma, Parco Area delle Scienze 7/a (Campus), 43124 Parma, Italy

^{d}*Dipartimento di Fisica and INFN, Università di Roma "Tor Vergata",*
  Via della Ricerca Scientifica 1, I-00133 Roma, Italy

^{j}*Institute for Theoretical Physics, Albert Einstein Center for Fundamental Physics,*
  University of Bern, Sidlerstrasse 5, CH-3012 Bern, Switzerland

^{e}*Istituto Nazionale di Fisica Nucleare, Sezione di Roma Tre,*
  Via della Vasca Navale 84, I-00146 Rome, Italy

^{f}*HISKP (Theory), Rheinische Friedrich-Wilhelms-Universität Bonn,*
  Nussallee 14-16, 53115 Bonn, Germany

^{g}*High Performance Computing and Analytics Lab, Rheinische Friedrich-Wilhelms-Universität Bonn,*
  Friedrich-Hirzebruch-Allee 8, 53115 Bonn, Germany

^{h}*NIC, DESY, Platanenallee 6, D-15738 Zeuthen, Germany*

^{i}*Dipartimento di Matematica e Fisica, Università Roma Tre and INFN, Sezione di Roma Tre,*
  Via della Vasca Navale 84, I-00146 Rome, Italy

  E-mail: s.bacchio@gmail.com

We present a lattice determination of the disconnected contributions to the leading-order hadronic vacuum polarization (HVP) to the muon anomalous magnetic moment in the so-called short and intermediate time-distance windows. We employ gauge ensembles produced by the Extended Twisted Mass Collaboration (ETMC) with $N_f = 2 + 1 + 1$ flavours of Wilson twisted-mass clover-improved quarks with masses approximately tuned to their physical value. We take the continuum limit employing three lattice spacings at about 0.08, 0.07 and 0.06 fm.

The 39th International Symposium on Lattice Field Theory (Lattice2022),
8-13 August, 2022
Bonn, Germany

---

*Speaker

1. Introduction

In Ref. [1] we have presented our full calculation of the short and intermediate time-distance hadronic vacuum polarization (HVP) contributions to the muon magnetic moment using twisted-mass fermions on ETMC ensembles. In this work, we present an extract that focuses on disconnected contributions, summarizing the results of the manuscript and providing some additional details.

In our calculation, we have adopted the time momentum representation [2] and evaluate the HVP contribution to the muon anomalous magnetic moment a_μ^{HVP} as

$$a_\mu^{\mathrm{HVP}} = 2\alpha_{em}^2 \int_0^\infty dt\, t^2\, K(m_\mu t)\, V(t) \,, \tag{1}$$

where t is the Euclidean time and the kernel function $K(m_\mu t)$ is defined as[1]

$$K(z) = 2 \int_0^1 dy(1-y)\left[1 - j_0^2\left(\frac{z}{2}\frac{y}{\sqrt{1-y}}\right)\right] \,, \qquad j_0(y) = \frac{\sin(y)}{y} \,. \tag{2}$$

The Euclidean vector correlator $V(t)$ is defined as

$$V(t) \equiv -\frac{1}{3}\sum_{i=1,2,3}\int d^3x\, \langle J_i(\vec{x}_f, t_f) J_i(\vec{x}_i, t_i)\rangle \tag{3}$$

with $J_\mu(x)$ being the electromagnetic current operator

$$J_\mu(x) \equiv \sum_{f=u,d,s,c,\dots} q_f\, \overline{\psi}_f(x)\gamma_\mu\psi_f(x) \tag{4}$$

and q_f the electric charge for the quark flavour f (in units of the absolute value of the electron charge). Clearly, the vector correlator $V(t)$ give rise to both connected and disconnected contributions, as depicted in Fig. 1. The latter are the focus of this proceeding.

Figure 1: *Connected (left) and disconnected (right) contributions to the vector correlator $V(t)$.*

1.1 The RBC/UKQCD windows in the time-momentum representation

Following the analysis of the RBC/UKQCD Collaboration [3], we separate the whole HVP contribution in three terms,

$$a_\mu^{\mathrm{HVP}} \equiv a_\mu^{\mathrm{SD}} + a_\mu^{\mathrm{W}} + a_\mu^{\mathrm{LD}} \,, \tag{5}$$

that can be obtained from Eq. (1) with integration kernel $K(m_\mu t)$ multiplied by suitably smoothed Heaviside step-functions, namely

$$a_\mu^w = 2\alpha_{em}^2 \int_0^\infty dt\, t^2\, K(m_\mu t)\, \Theta^w(t)\, V(t) \qquad w = \{\mathrm{SD}, \mathrm{W}, \mathrm{LD}\} \,, \tag{6}$$

---

[1]The leptonic kernel $K(z)$ is proportional to z^2 at small values of z and it goes to 1 for $z \to \infty$.

where the time-modulating function $\Theta^w(t)$ is given by

$$\Theta^{\text{SD}}(t) \equiv 1 - \frac{1}{1 + e^{-2(t-t_0)/\Delta}} , \tag{7}$$

$$\Theta^{\text{W}}(t) \equiv \frac{1}{1 + e^{-2(t-t_0)/\Delta}} - \frac{1}{1 + e^{-2(t-t_1)/\Delta}} , \tag{8}$$

$$\Theta^{\text{LD}}(t) \equiv \frac{1}{1 + e^{-2(t-t_1)/\Delta}} \tag{9}$$

with the parameters t_0, t_1, Δ chosen [3] to be equal to

$$t_0 = 0.4 \text{ fm} , \qquad t_1 = 1 \text{ fm} , \qquad \Delta = 0.15 \text{ fm} . \tag{10}$$

2. Lattice setup

In this work we compute disconnected contributions on three ensembles with $N_f = 2 + 1 + 1$ flavours of Wilson twisted-mass clover-improved quarks with masses approximately tuned to their physical value. The parameters of the ensembles are give in Table 1. For the full calculation in Ref. [1], a fourth ensemble, cB211.072.96, at $\beta = 1.778$ and lattice volume $V/a^4 = 96^3 \cdot 192$ was used for estimating finite size effects (FSEs). However, due to the high cost of the calculation, we did not compute disconnected contributions using the larger volume cB211.072.96 ensemble, since FSEs are expected to be within statistical errors.

ensemble	β	V/a^4	a (fm)	$a\mu_\ell$	M_π (MeV)	L (fm)	$M_\pi L$
cB211.072.64	1.778	$64^3 \cdot 128$	0.07961 (13)	0.00072	140.2 (0.2)	5.09	3.62
cC211.060.80	1.836	$80^3 \cdot 160$	0.06821 (12)	0.00060	136.7 (0.2)	5.46	3.78
cD211.054.96	1.900	$96^3 \cdot 192$	0.05692 (10)	0.00054	140.8 (0.2)	5.46	3.90

Table 1: *Parameters of the ETMC ensembles used in this work. We give the light-quark bare mass, $a\mu_\ell = a\mu_u = a\mu_d$, the pion mass M_π, of the lattice size L and the product $M_\pi L$.*

3. Noise reduction techniques and statistics

The disconnected contributions are computed for the light-, strange- and charm-quark masses. Various noise-reduction techniques are employed to improve the signal-to-noise ratio of disconnected loops. These are the one-end-trick [4], exact deflation of low-modes [5] and hierarchical probing [6]. The one-end-trick is used for all loops; hierarchical probing with distance 8 is used for all loops, except the charm-quark loops for the cB211.072.64 ensemble, where distance 4 is used; and deflation of the low-modes is used for the light quark loops for the cB211.072.64 and cC211.060.80 ensembles. The latter is not employed for the cD211.054.96 ensemble because of the prohibitively large memory requirements. Indeed, the number of low-modes to be deflated should be increased with the volume, making the costs of this technique to scale with volume-squared. For this reason deflation is not used on the larger volume and, instead, multiple stochastic sources

Flavour	cB211.072.64				cC211.060.80				cD211.054.96			
	N_{defl}	N_{r}	N_{Had}	N_{vect}	N_{defl}	N_{r}	N_{Had}	N_{vect}	N_{defl}	N_{r}	N_{Had}	N_{vect}
Light	200	1	512	6144	450	1	512	6144	0	8	512	49152
Strange	0	2	512	12288	0	4	512	24576	0	4	512	24576
Charm	0	12	32	4608	0	1	512	6144	0	1	512	6144
N_{confs}	×750 configurations				×400 configurations				×500 configurations			

Table 2: *Noise reduction techniques and statistics used for the disconnected quark loops. For each ensemble, the columns are in order: i) the number of deflated eigenvectors N_{defl}, ii) the number of stochastic sources N_{r}, iii) the number of Hadamard vectors N_{Had}, and iv) the total number of computed vectors $N_{\text{vect}} = 12 \times N_{\text{r}} \times N_{\text{Had}}$.*
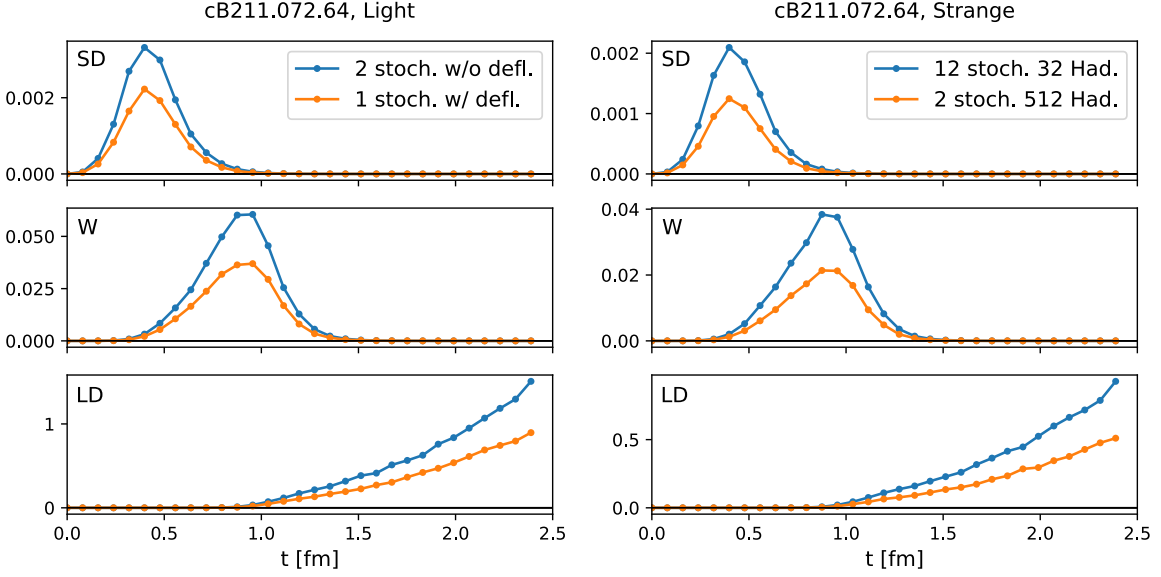
Figure 2: *Statistical errors of the integrand in the short (SD), intermediate (W) and long (LD) distance windows for the light (left panel) and strange (right panel) contributions to the disconnected loops on the cB211.072.64 ensemble. In orange are the values used in the final calculation, i.e. those reported in Table 2, while in blue are the same quantities computed with an alternative setup. Namely, we used 2 stochastic sources (instead of 1) but no deflation for the light loops and used 12 stochastic sources (instead of 2) and 32 Hadamard vectors (instead of 512) for the strange loops. In the text we report about the gain in cost-to-error.*

are utilized. In Table 2 we summarize the statistics used for the three ensembles and three quark flavours.

For certain flavour of quark loops we have also available a calculation made with a different setup. E.g. on the cB211.072.64, for the light disconnected contributions, we have also computed loops without deflation and two stochastic sources, or, for the strange disconnected contributions, we have employed 12 stochastic sources and 32 Hadamard vectors. These different combinations allow us to estimate the improvements due to the noise reduction techniques adopted. We analyse this in Fig. 2 where we compare the error on disconnected contributions for the various windows using the aforementioned statistics for the light- and strange-quark loops. Looking at the light-quark loops, the cost for one stochastic source with deflation is about 35% cheaper than computing two stochastic sources without deflation, and its error is also 35% smaller. Summing these up, deflation reduces the cost-to-error ratio by a factor of 3.7× for this specific quantity and ensemble. Looking

at the strange-quark loops, 2 sources with 512 Hadamard vectors require 2.7× more computational resources than 12 sources with 32 Hadamard vector and reduce the errors squared by a factor of 3×, resulting in a 11% reduction of the cost-to-error ratio.

4. The strange- and charm-quark loops

The strange- and charm-quark loops are computed at a quark mass obtained by tuning the Ω and Λ_c baryons, respectively, to their physical value. The values of the bare masses for the strange, $a\mu_s$, and for the charm, $a\mu_c$, quarks are listed in Table 3. In Fig. 3, we show the continuum limit of the renormalized strange and charm quark masses in the $\overline{MS}$(2 GeV) and $\overline{MS}$(3 GeV) scheme [7], respectively. We compare them against the results computed in the continuum limit in Ref. [7]. We note that the values of $a\mu_s$ do not show sizable cut-off effects, while $a\mu_c$ does.

Ensemble	$a\mu_s$	$a\mu_c$
cB211.072.64	0.01860	0.249
cC211.060.80	0.01615	0.206
cD211.054.96	0.01360	0.166

Table 3: *Values of the bare quark masses $a\mu_s$ and $a\mu_c$ used for the calculation of strange and charm disconnected contributions.*
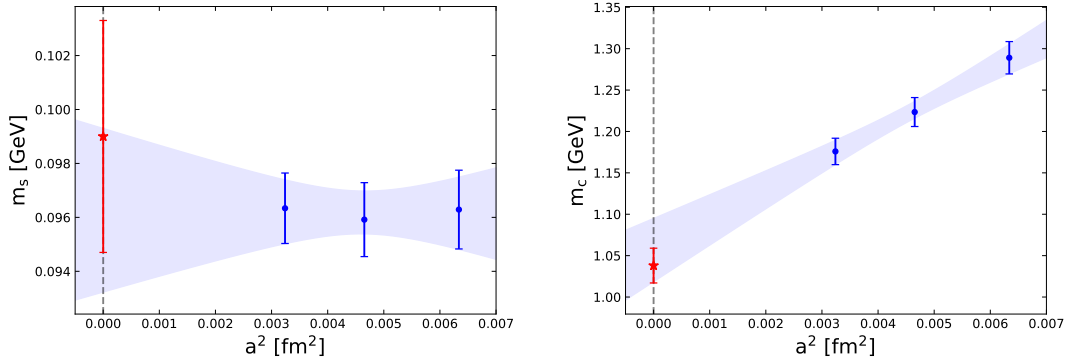
Figure 3: *Renormalized strange (left) and charm (right) quark mass, given respectively in the $\overline{MS}$(2 GeV) and $\overline{MS}$(3 GeV) scheme [7, 8], tuning the Ω and Λ_c baryon masses, versus the squared lattice spacing. The red stars are the results of the continuum limit extrapolation carried out in Ref. [7].*

5. Disconnected contributions

The quark disconnected contributions to the vector correlator $V(t)$ (see Eq. (3)) is the sum of the six relevant quark disconnected correlators weighted by the appropriate charge factors, namely

$$
\begin{aligned}
V_{\text{disc.}}(x) = \sum_{i=1,2,3} \Bigg(& + \frac{1}{9}\left\langle J_i^{\ell\ell}(x)[J_i^{\ell\ell}]^\dagger(0)\right\rangle + \frac{1}{9}\left\langle J_i^{ss}(x)[J_i^{ss}]^\dagger(0)\right\rangle + \frac{4}{9}\left\langle J_i^{cc}(x)[J_i^{cc}]^\dagger(0)\right\rangle \\
& - \frac{1}{9}\left\langle J_i^{\ell\ell}(x)[J_i^{ss}]^\dagger(0) + \text{hc}\right\rangle + \frac{2}{9}\left\langle J_i^{\ell\ell}(x)[J_i^{cc}]^\dagger(0) + \text{hc}\right\rangle - \frac{2}{9}\left\langle J_i^{ss}(x)[J_i^{cc}]^\dagger(0) + \text{hc}\right\rangle \Bigg),
\end{aligned}
$$

(11)

5

where the renormalized vector currents J_i^{ff}, which are written in terms of Osterwalder-Seiler valence lattice quarks [9, 10], read as

$$J_\mu^{\ell\ell}(x) = Z_V \bar{\ell}(x)\gamma_\mu \ell(x) , \quad J_\mu^{ss}(x) = Z_V \bar{s}(x)\gamma_\mu s(x) , \quad J_\mu^{cc}(x) = Z_V \bar{c}(x)\gamma_\mu c(x) . \quad (12)$$

For details on the calculation of the renormalization constant Z_V we refer to Ref. [1]. From the vector correlator $V_{disc.}(t)$ the values of $a_\mu^{\text{SD}}(disc.)$ and $a_\mu^{\text{W}}(disc.)$ are straightforwardly evaluated according to Eq. (6). The results for the diagonal and off-diagonal disconnected contributions are summarized in Table 4 for a_μ^{SD} and in Table 5 for a_μ^{W}.

Ensemble	$\ell\ell$	ss	cc	ℓs	ℓc	sc
cB211.072.64	−3.37 (13)	−2.090 (59)	−1.18 (14)	+5.29 (15)	−1.52 (24)	+1.67 (13)
cC211.060.80	−3.36 (16)	−2.090 (73)	−0.78 (11)	+5.53 (17)	−1.48 (20)	+1.37 (15)
cD211.054.96	−3.54 (16)	−2.084 (75)	−0.71 (14)	+5.60 (18)	−1.51 (21)	+1.27 (18)

Table 4: *Summary of the various flavour contributions to $a_\mu^{\text{SD}}(disc.)$ in units of 10^{-12} for the cB211.072.64, cC211.060.80 and cD211.054.96 ensembles. The symbols $\ell\ell$, ss and cc denote respectively the flavour-diagonal light, strange and charm contributions, while ℓs, ℓc and sc denote the off-diagonal light-strange, light-charm and strange-charm contributions, respectively.*

Ensemble	$\ell\ell$	ss	cc	ℓs	ℓc	sc
cB211.072.64	−1.087 (49)	−0.149 (22)	−0.030 (53)	+0.635 (58)	+0.00 (8)	−0.02 (6)
cC211.060.80	−1.300 (69)	−0.159 (27)	−0.033 (49)	+0.726 (81)	−0.03 (7)	+0.04 (7)
cD211.054.96	−1.201 (73)	−0.149 (29)	+0.018 (54)	+0.627 (81)	+0.02 (8)	−0.02 (7)

Table 5: *The same as in Table 4, but for the various flavour contributions to $a_\mu^{\text{W}}(disc.)$ in units of 10^{-10}.*

Ensemble	$a_\mu^{\text{SD}}(disc.)$	$a_\mu^{\text{W}}(disc.)$
cB211.072.64	$-1.20\ (23) \cdot 10^{-12}$	$-0.651\ (93) \cdot 10^{-10}$
cC211.060.80	$-0.80\ (18) \cdot 10^{-12}$	$-0.762\ (75) \cdot 10^{-10}$
cD211.054.96	$-0.96\ (20) \cdot 10^{-12}$	$-0.701\ (80) \cdot 10^{-10}$
Continuum	$-0.6\ (5) \cdot 10^{-12}$	$-0.78\ (21) \cdot 10^{-10}$

Table 6: *Final results for the disconnected contributions to the short and intermediate distance windows*

In Table 6 we give the sum of all contributions and the result of the continuum limit that we take as final value. In Fig. 4, we show the continuum limit extrapolation for the disconnected contributions to a_μ^{SD} and a_μ^{W}. Qualitatively, for a_μ^{W} the light-light contribute +150% of the total disconnected contribution, the strange-light -80% and the strange-strange +30%. All other combinations are consistent with zero within the errors. We do not observe sizable cutoff effects at this level of precision. The disconnected contribution to a_μ^{SD} is very small, being approximately forty times smaller as compared to our error on the light-connected contribution to a_μ^{SD}. Given the available data, we perform only two continuum extrapolation, using either a constant fit Ansatz or a linear one in a^2. The latter fit Ansatz is adopted in view of the expected automatic O(a) improvement [10] of the relevant two-point correlation functions of the renormalized vector currents in Eq. (12). The extrapolated values using these two fitting procedures are in agreement with each other. The one obtained from the linear fit in a^2 has a larger statistical uncertainty and conservatively we take it as our final estimate.
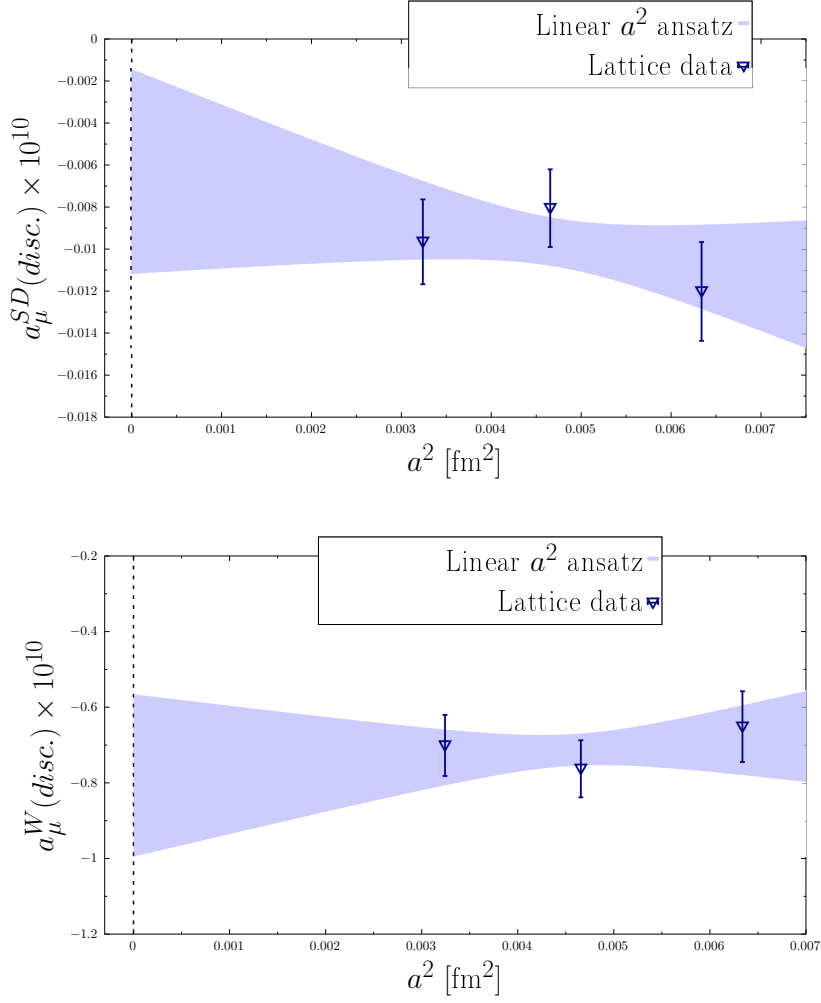
Figure 4: *Top panel: The quark-loop disconnected contribution to the short time-distance window, a_μ^{SD}, versus the squared lattice spacing a^2 in physical units. Bottom panel: the same as in the top panel, but for the intermediate window a_μ^{W}. The blue band corresponds to the extrapolation performed using a linear fit Ansatz in a^2.*

Ref.	$a_\mu^{\mathrm{W}}(disc.)$
this work	$-0.78\,(0.21) \cdot 10^{-10}$
BMW [11]	$-0.85\,(0.06) \cdot 10^{-10}$
CLS/Mainz [12]	$-0.81\,(0.09) \cdot 10^{-10}$
average	$-0.83\,(0.05) \cdot 10^{-10}$

Table 7: *Disconnected contribution to the intermediate time-distance window a_μ^{W} obtained in this work and in Refs. [11, 12]. The last row lists the average of all lattice results made following the PDG approach.*

6. Conclusions

In Table 7 we compare our results with those obtained by BMW [11] and CLS/Mainz [12] on the disconnected contribution to the intermediate window. The largest systematic effect on our error comes from the continuum extrapolation. We observe a remarkable agreement among all available lattice results. In the future we plan to extended this calculation with a further lattice spacing in order to improve our continuum extrapolation.

Acknowledgments

References

[1] C. Alexandrou et al., *Lattice calculation of the short and intermediate time-distance hadronic vacuum polarization contributions to the muon magnetic moment using twisted-mass fermions*, 2206.15084.

[2] D. Bernecker and H.B. Meyer, *Vector Correlators in Lattice QCD: Methods and applications*, *Eur. Phys. J. A* **47** (2011) 148 [1107.4388].

[3] RBC, UKQCD collaboration, *Calculation of the hadronic vacuum polarization contribution to the muon anomalous magnetic moment*, *Phys. Rev. Lett.* **121** (2018) 022003 [1801.07224].

[4] UKQCD collaboration, *Decay width of light quark hybrid meson from the lattice*, *Phys. Rev. D* **73** (2006) 074506 [`hep-lat/0603007`].

[5] A.S. Gambhir, A. Stathopoulos and K. Orginos, *Deflation as a Method of Variance Reduction for Estimating the Trace of a Matrix Inverse*, *SIAM J. Sci. Comput.* **39** (2017) A532 [`1603.05988`].

[6] A. Stathopoulos, J. Laeuchli and K. Orginos, *Hierarchical probing for estimating the trace of the matrix inverse on toroidal lattices*, `1302.4018`.

[7] Extended Twisted Mass collaboration, *Quark masses using twisted-mass fermion gauge ensembles*, *Phys. Rev. D* **104** (2021) 074515 [`2104.13408`].

[8] ETM collaboration, *Non-perturbative renormalisation of quark bilinear operators with $n_f = 2 + 1 + 1$ wilson-clover twisted-mass fermions*, .

[9] K. Osterwalder and E. Seiler, *Gauge Field Theories on the Lattice*, *Annals Phys.* **110** (1978) 440.

[10] R. Frezzotti and G.C. Rossi, *Chirally improving Wilson fermions. II. Four-quark operators*, *JHEP* **10** (2004) 070 [`hep-lat/0407002`].

[11] S. Borsanyi et al., *Leading hadronic contribution to the muon magnetic moment from lattice QCD*, *Nature* **593** (2021) 51 [`2002.12347`].

[12] M. Cè et al., *Window observable for the hadronic vacuum polarization contribution to the muon $g − 2$ from lattice QCD*, `2206.06582`.

[13] M.A. Clark, R. Babich, K. Barros, R.C. Brower and C. Rebbi, *Solving Lattice QCD systems of equations using mixed precision solvers on GPUs*, *Comput. Phys. Commun.* **181** (2010) 1517 [`0911.3191`].

[14] R. Babich, M.A. Clark, B. Joo, G. Shi, R.C. Brower and S. Gottlieb, *Scaling Lattice QCD beyond 100 GPUs*, in *SC11 International Conference for High Performance Computing, Networking, Storage and Analysis Seattle, Washington, November 12-18, 2011*, 2011, DOI [`1109.2935`].

[15] M.A. Clark, B. Joó, A. Strelchenko, M. Cheng, A. Gambhir and R.C. Brower, *Accelerating Lattice QCD Multigrid on GPUs Using Fine-Grained Parallelization*, in *SC '16: Proceedings of the International Conference for High Performance Computing, Networking, Storage and Analysis*, pp. 795–806, 2016, DOI [`1612.07873`].

[16] Jülich Supercomputing Centre, *JUWELS: Modular Tier-0/1 Supercomputer at the Jülich Supercomputing Centre*, *Journal of large-scale research facilities* **5** (2019) .

[17] Jülich Supercomputing Centre, *JURECA: Modular supercomputer at Jülich Supercomputing Centre*, *Journal of large-scale research facilities* **4** (2018) .